Anal. Chem. **2000,** *72,* 680−686

Electrode Coatings Based on Chitosan Scaffolds

Juan Cruz, Michelle Kawasaki, and Waldemar Gorski*

Division of Earth and Physical Sciences, The University of Texas at San Antonio, San Antonio, Texas 78249-0663

Thin films of a biopolymer chitosan (CHIT) were cast on glassy carbon electrodes, modified by grafting Lucifer Yellow VS dye (LYVS) onto chitosan chains, and cross-linked with glutaric dialdehyde (GDI). The ion-transport and ion-exchange properties of such polymeric structures (CHIT, CHIT-LYVS, CHIT-LYVS-GDI) were studied using cyclic voltammetry, rotating disk electrode, and flow injection analysis. The results showed that the chitosan matrix supported a fast ion transport as demonstrated by aqueous-like values of the apparent diffusion coefficients of $Ru(NH_3)_6^{3+}$ and dopamine in the films. Anionic LYVS dye introduced a permselectivity against anions (e.g., $Fe(CN)_6^{4-}$, ascorbate) into the CHIT-LYVS films. The cross-linking of such films with GDI further increased their permselectivity as well as their stability. A unique combination of high permselectivity and fast ion transport in the CHIT-LYVS-GDI films is discussed in terms of the mixed-transport mechanism involving both pore and membrane diffusion in a highly hydrated chitosan matrix. The results indicate that the chemically modified chitosan is an attractive new coating for the development of fast, selective, and reversible sensors.

With this paper we initiate a systematic exploration of a natural polymer, chitosan, as a structural material for designing functional layers on electrode surfaces. Chitosan is a N-deacetylated derivative of chitin, a naturally occurring biopolymer found in the exoskeleton of crustaceans, in fungal cell walls, and in other biological material.[1] We have selected chitosan because of an unusual combination of its properties,[2] which include excellent membrane-forming ability, high permeability toward water, good adhesion, biocompatibility, nontoxicity, high mechanical strength, and susceptibility to chemical modifications due to the presence of reactive amino and hydroxyl functional groups. These properties prompted extensive investigations of chitosan in the past. For example, chitosan has been studied[1−3] as a material for contact lens, as a matrix for cell and enzyme immobilization, and as an artificial skin (e.g., chitosan−collagen composite). However, despite its attractive properties chitosan has received only very limited attention as a material for the design of modified electrodes.[4−7] A modification of electrodes with cellulose, which is structurally similar to chitosan, has been investigated more extensively.[8−13] Cellulose coatings have been studied primarily as a means to prevent electrode surface fouling and to exclude large interferences.

In the present study, a modification of electrodes with thin films of chitosan is described. The chitosan is used to control the access of ionic species to the electrode surface. Three types of chitosan films are studied: (1) films of unmodified chitosan (CHIT), (2) films made of chitosan that was chemically modified with the Lucifer Yellow VS dye (CHIT-LYVS), and (3) films of chitosan modified with LYVS and cross-linked with glutaric dialdehyde (CHIT-LYVS-GDI). The ion-transport and ion-exchange properties of such films were probed with both cationic ($Ru(NH_3)_6^{3+}$, dopamine) and anionic ($Fe(CN)_6^{4-}$, ascorbate) species using electrochemical techniques. Results of the spectrophotometric studies of the chitosan modified with LYVS dye are presented as well.

EXPERIMENTAL SECTION

Chemicals. The chemicals were of the highest quality commercially available and were used without further purification. Chitosan (MW $1.9-3.1 \times 10^5$; 75−85% deacetylation), Lucifer Yellow VS dye (dilithium 4-amino-*N*-[3-(vinylsulfonyl)phenyl]-naphthalimide-3,6-disulfonate), glutaric dialdehyde (50 wt % solution in H_2O), $Ru(NH_3)_6Cl_3$, L-ascorbic acid, and dopamine were purchased from Aldrich. Other chemicals such as $K_4Fe(CN)_6$, $NaH_2PO_4 \cdot H_2O$, NaCl, and NaOH were from Fisher. Solutions were prepared using deionized water which was purified with a Barnstead NANOpure cartridge system. Water used for preparation of dopamine and ascorbate solutions was deoxygenated with argon.

Electrochemical Techniques and Data Collection. Cyclic voltammetry, rotating-disk voltammetry, and flow injection amperometry was performed with the BAS (Bioanalytical Systems, Inc.) model 100B/W workstation and a BAS rotating-disk electrode model RDE-1 (software version 2.1). Experiments were performed at room temperature (21 ± 1 °C) in a conventional three-electrode system with 3-mm-diameter glassy carbon working electrode (BAS) and a platinum wire as the auxiliary electrode.

* Corresponding author: (fax) 210-458-4469; (e-mail)wgorski@utsa.edu.

(1) Peter, M. G. *J. M. S.-Pure Appl. Chem.* **1995**, *A32*, 629−640.
(2) Muzzarelli, R. A. A. *Chitin*; Pergamon Press: Oxford, 1977.
(3) Sandford, P. A. In *Chitin and Chitosan*; Skjak-Braek, G., Anthonsen, T., Sandford, P., Eds.; Elsevier: London, 1989.
(4) Hikima, S.; Kakizaki, T.; Taga, M.; Hasebe, K. *Fresenius J. Anal. Chem.* **1993**, *345*, 607−609.
(5) Zhao, C.-Z.; Egashira, N.; Ohga, K. *Anal. Sci.* **1998**, *14*, 439−443.
(6) Jinrui, X.; Bin, L. *Analyst* **1994**, *119*, 1599−1601.
(7) Ye-, X.; Yang, Q.; Wang, Y.; Li, N. *Talanta* **1998**, *47*, 1099−1106.
(8) Sittampalam, G.; Wilson, G. S. *Anal. Chem.* **1983**, *55*, 1608−1610.
(9) Wang, J.; Hutchins, L. D. *Anal. Chem.* **1985**, *57*, 1536−1541.
(10) Wang, J.; Tuzhi, P. *Anal. Chem.* **1986**, *58*, 3257−3261.
(11) Hutchins-Kumar, L. D.; Wang, J.; Tuzhi, P. *Anal. Chem.* **1986**, *58*, 1019−1023.
(12) Wang, J.; Tuzhi, P. *J. Electrochem. Soc.* **1987**, *134*, 586−591.
(13) Kuhn, L. S.; Weber, G. S.; Ismail, K. Z. *Anal. Chem.* **1989**, *61*, 303−309.

10.1021/ac990954b CCC: $19.00
Published on Web 01/19/2000

The glassy carbon electrodes were polished prior to the experiments on an Alpha A polishing cloth (Mark V Lab) with successively smaller particles (0.3- and 0.05-μm diameter) of alumina suspended in deionized water. After each polishing step the slurry accumulated on the electrode surface was removed by a 1-min ultrasonication in deionized water. The reference electrode was Ag/AgCl/3 M NaCl (BAS). All experiments were repeated at least three times and the means of measurements are presented with the standard deviations.

Spectroscopic and Scanning Electron Microscopy Measurements. Electronic spectra of LYVS in pH 7.40 phosphate buffer were recorded with the HP-8453 UV/visible diode array spectrophotometer using a cuvette with a path length of 1 cm. The chitosan films were prepared on quartz slides following the procedures described below and were always dried at room temperature before measurements. Scanning electron microscope microphotographs of chitosan films, prepared on glassy carbon rods, were made with a JEOL 840A scanning electron microscope.

Preparation of Chitosan Films. The CHIT films of unmodified chitosan were prepared by the casting technique. A 1.0 wt % chitosan solution was prepared by dissolving chitosan flakes in hot 0.05 M HCl. The solution was cooled to room temperature and filtered using a 0.45-μm Millex-HA syringe filter unit (Millipore). In a typical casting procedure, 20 μL of 0.10 wt % chitosan solution was placed on the substrate and allowed to evaporate for 1 h at room temperature. This procedure resulted in a transfer of ~20 μg of chitosan, which, considering that on average 80% of chitosan is deacetylated, corresponds to 9.9×10^{-8} mol of glucosamine units (FW = 161 g mol^{-1}). The CHIT film was neutralized in 0.10 M NaOH and conditioned in pH 7.40 phosphate buffer solution for 1 h before use.

The chitosan coatings containing LYVS were obtained by a solid-phase modification of CHIT films. Such an approach was chosen because attempts to produce a homogeneous casting solution by mixing chitosan and LYVS resulted in the formation of a precipitate. The CHIT-LYVS films were obtained by soaking the CHIT films in 3.0 mM LYVS solution buffered at pH 7.40 for 17 h. CHIT-LYVS films were cross-linked in 10.0 wt % glutaric dialdehyde solution for 2 h; this produced the CHIT-LYVS-GDI films. The average thickness of dry chitosan films was 2.0 ± 0.2 μm as determined by scanning electron microscopy of their cross sections.

Determination of Apparent Diffusion Coefficients of Cationic Redox Probes in Chitosan Films. Diffusion coefficients of $Ru(NH_3)_6^{3+}$ and dopamine were measured with a rotating-disk electrode (RDE) covered with a chitosan film. The limiting current I_L due to the redox of the probe at a film-covered RDE can be described by the equation[14−16]

$$I_L^{-1} = \delta_f(nFAC_sD_{app})^{-1} + (0.62nFAC_sD_s^{2/3}\nu^{-1/6})^{-1}\omega^{-1/2} \quad (1)$$

where δ_f is the film thickness (cm), A is the electrode area (cm^2), C_s is the concentration of the redox probe in the solution (mol cm^{-3}), $D_{app} = \alpha D_f$, $\alpha = C_f/C_s$ is the probe's partition coefficient where C_f is the concentration of the probe in the film, D_f is the probe's diffusion coefficient in the film, ν is the kinematic viscosity of the solution (cm^2 s^{-1}), ω is the angular velocity of electrode rotation (rad s^{-1}), D_s is the probe's diffusion coefficient in the solution (cm^2 s^{-1}), and n and F have their usual meaning. The first and second terms on the right-hand side of eq 1 represent the rate of a probe transfer in the film and in the solution layer adjacent to the film, respectively. The apparent diffusion coefficients D_{app} were obtained from the intercepts of plots I_L^{-1} vs $\omega^{-1/2}$. The values of D_{app} were considered a minimum, since the dry film thickness δ_f was used in calculations. Some increase in δ_f for wet films can be expected because of the film swelling in the solution.

Partition of Cationic Probes Between Chitosan Films and a Solution. To obtain D_f from D_{app}, the partition coefficients α of the probes were determined independently by using a coulometric assay of the electrode covered with a chitosan film. The electrode was equilibrated for 30 min with a stirred solution of a redox probe and then transferred to a pure supporting electrolyte where a linear scan voltammogram was recorded after a specified delay time. The voltammetric peak current decreased with an increase in a delay time, indicating a departure of the redox probe from the film at the open circuit. To correct for this loss, the peak currents were integrated and the charges thus obtained were extrapolated to delay time zero yielding the initial charge $Q_{t=0}$, which corresponded to the number of moles of the redox probe partitioned into the film. The charge $Q_{t=0}$ was used to calculate the partition coefficient α using the following expression

$$\alpha = [Q_{t=0}(nFV_f)^{-1}]/C_s \quad (2)$$

where V_f is a volume of the chitosan film (dm^3) and $C_s = 1.0 \times 10^{-4}$ M. Experiments done with buffer solutions at pH 7.40 and 12.00 yielded values of α similar within ±20%.

RESULTS AND DISCUSSION

Chemical Modifications of Chitosan Films. Chitosan is a linear copolymer of glucosamine and *N*-acetylglucosamine (Figure 1A). In acidic solutions, chitosan behaves as a cationic polyelectrolyte ($pK_a = 6.3$).[17] Due to the deprotonation of amine groups at higher pH, dissolved chitosan usually flocculates at pH >6.[18] By evaporating water from acidic solutions of chitosan, strong chitosan membranes are easily formed due to the presence of hydrogen bonds between the hydroxyl groups, amino groups, and hydroxyl and amino groups.

Chitosan films were modified with anionic LYVS dye (Figure 1B) in order to introduce a permselectivity against anions. The LYVS molecules contain activated vinyl groups that are known to undergo nucleophilic addition with amine groups under neutral conditions.[19] Indeed, this is the basis of wool dyeing with a number of reactive dyes. A reaction between the vinyl sulfone functionality

(14) Gough, D. A.; Leypoldt, J. K. *Anal. Chem.* **1979**, *51*, 439−444.
(15) Ikeda, T.; Schmehl, P.; Denisevich, K. W.; Murray, R. W. *J. Am. Chem. Soc.* **1982**, *104*, 2683−2691.
(16) Leddy, J.; Bard. A. J.; Maloy, J. T.; Saveant, J. M. *J. Electroanal. Chem.* **1985**, *187*, 205−227.
(17) Hawley, M. D.; Tatawadi, S. V.; Piekarski, S.; Adams, R. N. *J. Am. Chem. Soc.* **1967**, *89*, 447−450.
(18) Rinaudo, M.; Domard, A. In *Chitin and Chitosan*; Skjak-Braek, G., Anthonsen, T., Sandford, P., Eds.; Elsevier: London, 1989; p 71.
(19) Stewart, W. W. *Nature* **1981**, *292*, 17−21.

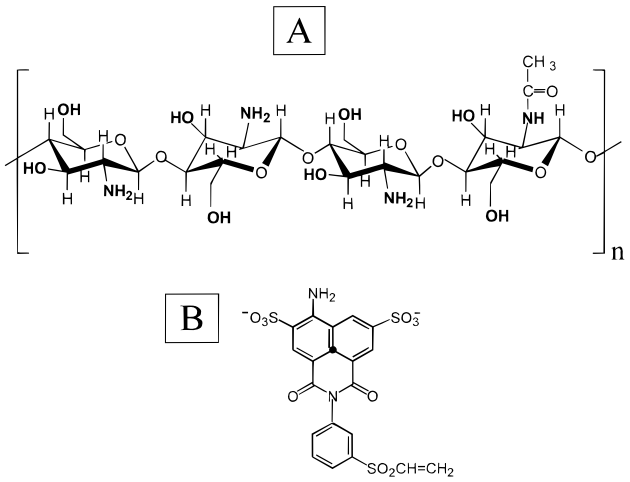

Figure 1. Chemical structures of chitosan (A) and Lucifer Yellow VS (B).

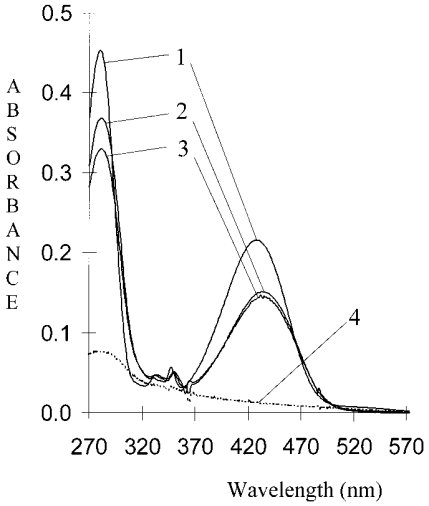

Figure 2. UV/visible spectrum of 0.020 mM LYVS in pH 7.40 phosphate buffer (1), and the spectra of dry chitosan films: CHIT-LYVS-GDI (2), CHIT-LYVS (3), and CHIT-GDI (4).

of LYVS and the amine group of chitosan can be represented by the equation

$$\mathrm{LY{-}SO_2{-}\mathbf{CH{=}CH_2} + \mathbf{NH_2}{-}CHIT \rightarrow LY{-}SO_2{-}\mathbf{CH_2{-}CH_2{-}NH}{-}CHIT}$$

where LY stands for Lucifer Yellow.

The immobilization of the LYVS in the chitosan films was examined by UV/visible spectrophotometry. The LYVS dye has two absorption bands located at 435 and 280 nm (Figure 2, curve 1) when dissolved in the buffer solution, agreeing with literature.[19] These bands are also present in the spectra of CHIT-LYVS and CHIT-LYVS-GDI dry films (Figure 2, curves 2 and 3). This confirms the presence of LYVS in the modified chitosan films since no absorption band is observed at 435 nm in the spectrum of a LYVS-free chitosan film (Figure 2, curve 4). Furthermore, the maximum absorbance values on curves 2 and 3 are practically the same, i.e., $A_{435} = 0.14 \pm 0.02$ AU, which suggests that both films contain the same amount of LYVS. The immobilization of

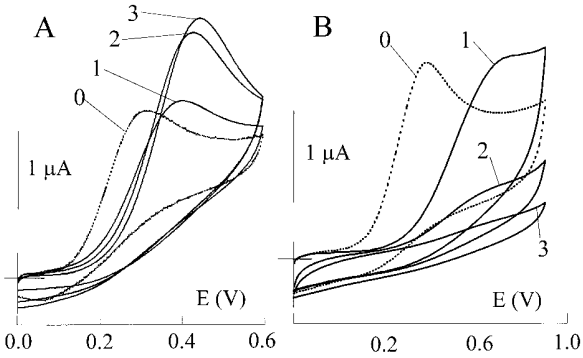

Figure 3. Cyclic voltammograms recorded in 0.10 mM solutions of dopamine (A) and ascorbate (B), at a bare glassy carbon electrode (0), and the electrode coated with CHIT (1), CHIT-LYVS (2), and CHIT-LYVS-GDI film (3). Background electrolyte, pH 7.40 phosphate buffer. Scan rate, 50 mV s^{-1}.

the dye in a chitosan matrix is strong because repetitive soaking and drying of the films did not diminish their maximum absorbance, which remained stable within ±5%.

The amount of LYVS immobilized in CHIT-LYVS and CHIT-LYVS-GDI films was determined by using a calibration curve. The calibration plot was constructed by measuring the UV/visible spectra of reference chitosan films loaded with known amounts of LYVS. Four reference films were prepared by pipetting 5.0, 10.0, 15.0, and 20.0 μL of 3.0 mM LYVS solution on top of the CHIT films and allowing the solvent to evaporate. The reference films were not soaked in a solution in order to prevent any loss of LYVS. A linear least-squares fit of the film absorbance at 435 nm vs micromoles of LYVS pipetted on the film yielded the calibration plot with a slope of 4.3 ± 0.3 AU μmol^{-1}, an intercept of 0.003 ± 0.001 AU, and a correlation coefficient of 0.991. According to the calibration plot, the absorbance $A_{435} = 0.14 \pm 0.02$ AU (Figure 2) corresponds to the presence of $(3.2 \pm 0.5) \times 10^{-8}$ mol of LYVS in chitosan films. A comparison of the latter number with the amount of chitosan glucosamine units on the substrate surface (9.9×10^{-8} mol) indicates that the molar ratio of LYVS to monomer units in the films is approximately 1:3.

Chitosan films were cross-linked with GDI in order to further modify their permeability to diffusing species. The cross-linking chemistry of chitosan with GDI is well known[20] and involves Schiff base formation according to the reaction

$$\mathrm{CHIT{-}N\mathbf{H_2} + \mathbf{O}{=}CH{-}(CH_2)_3{-}HC{=}O + \mathbf{H_2}N{-}CHIT \rightarrow CHIT{-}N{=}CH{-}(CH_2)_3{-}HC{=}N{-}CHIT + 2\mathbf{H_2O}}$$

The infrared spectroscopic studies of chitosan films, performed in order to determine the extent of cross-linking with GDI, were inconclusive. However, the extent of the cross-linking can be easily controlled since it is proportional to the reaction time and the concentration of the cross-linker. Heavily cross-linked chitosan films were of limited use as electrode coatings because they were impermeable to all four redox probes.

Influence of Chitosan Coatings on Electrode Processes of Selected Redox Systems. Figures 3 and 4 show cyclic voltammograms for the control bare glassy carbon electrode and

(20) Roberts, G. A. F.; Taylor, K. E. *Makromol. Chem.* **1989**, *190*, 951−958.

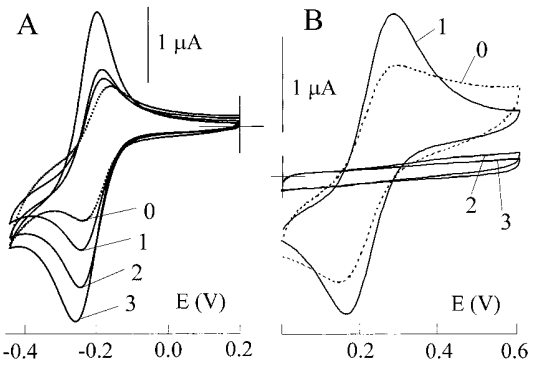

Figure 4. Cyclic voltammograms recorded in 0.10 mM solutions of $Ru(NH_3)_6^{3+}$ (A) and $Fe(CN)_6^{4-}$ (B), at a bare glassy carbon electrode (0), and the electrode coated with CHIT (1), CHIT-LYVS (2), and CHIT-LYVS-GDI film (3). Background electrolyte, pH 7.40 phosphate buffer. Scan rate, 50 mV s^{-1}.

for the electrodes coated with chitosan films in equilibrium with solutions containing dopamine, ascorbate, $Ru(NH_3)_6^{3+}$, and $Fe(CN)_6^{4-}$ ions. An overview of the voltammograms indicates that the chitosan coatings influence the electrode processes of these systems in two ways. First, the coatings either enhance or diminish the voltammetric peak currents of the redox probes, depending on the charge of the probe and the chemical modification of the chitosan matrix. This is discussed later (see section on Permeability of Chitosan Films) in terms of partitioning of the probes into or out of the electrode coatings.

A second affect of chitosan films is on the peak potentials of the redox probes, and it can be rationalized by influence of chitosan on the electrode kinetics. Figure 3 shows that the anodic peak potentials of both dopamine and ascorbate shift toward more positive values upon coating the electrode surface with chitosan films. Since oxidation of dopamine and ascorbate is chemically irreversible at the bare electrode, such a change in the peak potentials reflects a further inhibition of the electrode process by chitosan coatings. The oxidation of dopamine and ascorbate is a multistep electrode process involving the loss of two electrons and protons to produce dopamine-*o*-quinone and dehydroascorbate, respectively. Any of these steps may be adversely affected by the adsorption of chitosan at the electrode/solution interface. For example, the hydrogen bonding between dopamine, or ascorbate, and the chitosan matrix could result in the unfavorable orientation of their electroactive OH groups for electrooxidation and, thus, slow the kinetics of the electrode process.

On the other hand, the electron transfer in the simple one-electron redox systems such as $Ru(NH_3)_6^{3+/2+}$ and $Fe(CN)_6^{4-/3-}$ is not inhibited by the chitosan coatings. This conclusion is supported by the voltammetric data in Figure 4, which show that the anodic and cathodic peak potentials of these probes are practically the same at the bare electrode and at the electrodes coated with chitosan films. Further, the scan rate dependence of the peak potentials and peak currents of the $Ru(NH_3)_6^{3+/2+}$ and $Fe(CN)_6^{4-/3-}$ redox systems was not influenced by coating the electrodes with chitosan films (data not shown). Such behavior indicates that the chitosan coatings do not introduce any extra complications, e.g., due to the uncompensated film resistance.

Ion Transport in Chitosan Films. The ion transport in chitosan films was probed with two cationic redox species, $Ru(NH_3)_6^{3+}$ and dopamine, using the rotating-disk electrode. The electrodes were coated with a chitosan film, and S-shaped voltammograms were recorded in the probe solution at different rotation rates, ω. The limiting currents I_L on voltammograms were practically independent of potential and increased with ω. The plots I_L^{-1} vs $\omega^{-1/2}$ (eq 1) were linear with correlation coefficients ranging from 0.995 to 0.999. The slopes of such plots were equal to $(1.8 \pm 0.1) \times 10^6$ and $(2.1 \pm 0.1) \times 10^6$ A^{-1} $rad^{1/2}$ $s^{-1/2}$ for 0.2 mM $Ru(NH_3)_6^{3+}$ and 0.1 mM dopamine, respectively, at all electrodes. Their intercepts were equal to $(4.3 \pm 0.3) \times 10^4$, $(6.4 \pm 0.6) \times 10^4$, and $(1.1 \pm 0.2) \times 10^5$ A^{-1} for 0.2 mM $Ru(NH_3)_6^{3+}$, and $(6.7 \pm 0.6) \times 10^4$, $(1.1 \pm 0.2) \times 10^5$, and $(1.6 \pm 0.3) \times 10^5$ A^{-1} for 0.1 mM dopamine at the CHIT, CHIT-LYVS, and CHIT-LYVS-GDI electrodes, respectively. As anticipated from eq 1, the slopes and intercepts decreased with an increase in C_s, while an increase in the film thickness δ_f caused an increase in the intercept of the plot. These observations justified the use of eq 1 and the intercepts to calculate the apparent diffusion coefficients D_{app} of the $Ru(NH_3)_6^{3+}$ and dopamine in chitosan films.

Table 1 presents the D_{app} together with the diffusion coefficients D_s for these probes in the buffer solution. The coefficients D_s were calculated using eq 1 and slopes of the plot I_L^{-1} vs $\omega^{-1/2}$. The values of D_{app} in the films are of the same order of magnitude as those of D_s in the solution, which indicates a relatively unimpeded overall transport of cationic probes through chitosan films.

Table 1 also contains the partition coefficients α of $Ru(NH_3)_6^{3+}$ and dopamine into the chitosan films. Using the data in Table 1, one can now separate the two processes that control the overall transport of the probe through the film, i.e., the probe's partition in the film (α) and its diffusion within the film (D_f). Since $D_{app} = \alpha D_f$, the diffusion coefficients D_f were calculated by dividing D_{app} by α. Table 1 shows that the values of D_f are the highest in the CHIT film and decrease in the CHIT-LYVS and CHIT-LYVS-GDI films.

The condition that $D_f < D_s$ is an indication of chitosan films acting as a transport barrier that impedes diffusion of the probes to the surface of the glassy carbon electrode. The transport mechanism[21] could involve the diffusion through the pores in the film, a membrane-like diffusion through the bulk of the film, or a mixture of both pore and membrane diffusion. The pore mechanism is feasible because the chitosan films contain water-filled pores. The pores fluctuate in volume, are not fixed in definite location,[22] and have an average radius in the range from 9 to 18 Å, depending on the method of determination.[23] Although the two limiting mechanisms, pore and membrane diffusion, result in a similar form of I_L^{-1} vs $\omega^{-1/2}$ relationship,[16,24] they can be distinguished by the examination of the D_f and α coefficients.

The pore mechanism assumes that the probe transport occurs by diffusion in the bulk-like water of the pore. Thus, the probe diffusion coefficient in the film, D_f, should be close to that in the

(21) Wisniewski, S. J.; Gregonis, D. E.; Kim, S. W.; Andrade, J. D. In *Hydrogels for Medical and Related Applications*; Andrade, J. D., Ed.; ACS Symposium Series 31; American Chemical Society: Washington, DC, 1976; p 80.
(22) Yasuda, H.; Lamaze, C. E.; Ikenberry, L. D. *Makromol. Chem.* **1968**, *118*, 19−24.
(23) Zaborska, W.; Krajewska, B.; Leszko, M. *J. Membr. Sci.* **1991**, *61*, 279−288.
(24) McCarley, R. L.; Irene, E. A.; Murray, R. W. *J. Phys. Chem.* **1991**, *95*, 2492−2498.

Table 1. Apparent Diffusion Coefficients D_{App}, Partition Coefficients α, and Film Diffusion Coefficients D_f, for $Ru(NH_3)_6^{3+}$ and Dopamine in Chitosan Films and in Solution

	$Ru(NH_3)_6^{3+}$			dopamine		
film/probe	D_{app} ($\times 10^6$ cm^2 s^{-1})	α	D_f ($\times 10^6$ cm^2 s^{-1})	D_{app} ($\times 10^6$ cm^2 s^{-1})	α	D_f ($\times 10^6$ cm^2 s^{-1})
solution	5.1 ± 0.2[a]	1.0[b]	5.1 ± 0.2[a]	4.2 ± 0.2[a]	1.0[b]	4.2 ± 0.2[a]
CHIT	3.4 ± 0.3	2.9 ± 0.6	1.2 ± 0.3	2.2 ± 0.3	2.7 ± 0.6	0.8 ± 0.2
CHIT-LYVS	2.3 ± 0.2	8 ± 1	0.29 ± 0.04	1.3 ± 0.2	10 ± 1	0.13 ± 0.02
CHIT-LYVS-GDI	1.3 ± 0.1	20 ± 2	0.065 ± 0.008	0.9 ± 0.1	17 ± 2	0.053 ± 0.008

[a] Diffusion coefficient D_s in a solution determined from the slope of a plot I_L^{-1} vs $\omega^{-1/2}$ (see eq 1). [b] In a solution, $\alpha = 1.0$ by definition.

solution, D_s. Further, the partition coefficient α should be close to 1 since the probe is partitioning between the bulk aqueous solution and the bulk-like water in the pores. Table 1 shows that the values of D_f in the CHIT film are of the same order of magnitude as those determined in the buffer solution. In addition, the α values for the CHIT film are close to 1 and are the lowest of the three chitosan films. Thus, one can assume that the pore mechanism is the primary mode of operation in the CHIT film. A decrease of D_f in the chemically modified chitosan films can be ascribed to (1) the stronger electrostatic interactions of the cationic probes with the negatively charged pore walls in the CHIT-LYVS films and (2) a decrease in the pore size in the CHIT-LYVS-GDI film caused by the film cross-linking.[23] However, the slower diffusion in the CHIT-LYVS-GDI film can also be explained by a lower degree of hydration[25] of the chitosan matrix cross-linked with the hydrophobic GDI. The latter interpretation can also be used to explain a slower diffusion of ions that partition into the bulk of the film according to the membrane-like transport mechanism. Membrane-like partitioning of the probes is indeed observed in the CHIT-LYVS and CHIT-LYVS-GDI films as indicated by the increasing values of the α coefficients (Table 1). In conclusion, we believe that the probes are transported predominantly by the pore mechanism in the CHIT film and by the mixed mechanism involving both pore and membrane diffusion in chemically modified CHIT-LYVS and CHIT-LYVS-GDI films.

Ion transport in chitosan films is faster than in the Nafion films that are routinely used as coatings for electrochemical sensors. For example, the diffusion coefficients D_f of the $Ru(NH_3)_6^{3+}$ and dopamine in the CHIT-LYVS-GDI coatings (Table 1) are on average 1.5 orders of magnitude larger than in Nafion films.[26,27] The faster diffusion in chitosan than in Nafion can be explained by considering the structural differences between these polymers. While Nafion has a hydrophobic fluorocarbon backbone, the chitosan chains are hydrophilic since they are made of glucosamine units.[1,2] The better hydration of the hydrophilic chitosan matrix than that of the Nafion is probably responsible for the faster ionic diffusion in the CHIT-LYVS-GDI film. The importance of matrix hydration in controlling the rate of diffusion in chitosan membranes was recently demonstrated.[25]

Permeability of Chitosan Films. The voltammograms in Figures 3 and 4 were used to determine the permeability of the chitosan films to the four probes. The permeability, *P*, of a film to the redox probes was calculated from the following expression

$$P = (I_{film}/I_{bare}) \times 100\% \quad (3)$$

where I_{film} and $I_{bare}$are the voltammetric peak currents recorded at the film-coated electrode and the bare electrode, respectively. In the calculations, the anodic peak currents were used in the case of the dopamine, ascorbate, and $Fe(CN)_6^{4-}$, while the cathodic peak current was employed for the $Ru(NH_3)_6^{3+}$ probe. The coefficients of variation for the determination of film permeability *P* were on average ±10%.

Figure 5 (bars 1a−d) shows that the unmodified CHIT film has a good permeability ($P = 100-150\%$) to both the cationic and anionic probes. The analysis of such a behavior should take into account that the permeability, as defined by eq 3, is a function of the film's influence on the probe's diffusion, electrode kinetics, and partitioning. Generally, the slower ionic diffusion in the polymer than in water, and the slower kinetics at the electrode coated with the CHIT film (e.g., for dopamine and ascorbate) should cause the permeability *P* to be smaller than 100%. However, $P \geq 100\%$ indicates that the permeability is dominated by the preferential partitioning of the probes into the CHIT film. The hydrogen bond formation between the probes and the chitosan matrix is a probable driving force behind the probe partition into the CHIT film.

The chemical modification of the CHIT matrix with anionic LYVS dye introduces a charge-based molecular recognition to the chitosan coatings (Figure 5). The chemically modified films, CHIT-LYVS and CHIT-LYVS-GDI, display an increased permeability to cations ($P = 144-210\%$) and a greatly decreased permeability to anions ($P = 2-19\%$).

The increase in permeability of chitosan films to cationic probes, represented by the increase in current ratio I_{film}/I_{bare} (Figure 5, bars a and b), can indeed be explained in terms of the partition coefficient α as illustrated by the following calculations. Since the cyclic voltammetric peak currents I_{film} and I_{bare} are proportional to $C_f D_f^{1/2}$ and $C_s D_s^{1/2}$,[28] respectively, the current ratio I_{film}/I_{bare} can be expressed as $\alpha D_f^{1/2} D_s^{-1/2}$. Using the data in Table 1, the product ($\alpha D_f^{1/2} D_s^{-1/2}$) × 100% was found to be equal to 141, 190, and 226% for the $Ru(NH_3)_6^{3+}$ ions, and 119, 176, and 191% for dopamine at the CHIT, CHIT-LYVS, and CHIT-LYVS-GDI electrodes, respectively. These values are close to the current ratios I_{film}/I_{bare} for the two probes shown in Figure 5. That the experimental ratios I_{film}/I_{bare} for dopamine are smaller than the calculated product ($\alpha D_f^{1/2} D_s^{-1/2}$) × 100% can be ascribed to the increased irreversibility of the electrode process at chitosan electrodes.

(25) Nakatsuka, S.; Andrady, L. A. *J. Appl. Polym. Sci.* **1992**, *44*, 17−28.
(26) Martin, C. R.; Dollard, K. A. *J. Electroanal. Chem.* **1983**, *159*, 127−135.
(27) Kristensen, E. W.; Kuhr, W. G.; Wightman, R. M. *Anal. Chem.* **1987**, *59*, 1752−1757.
(28) Bard, A. J.; Faulkner, L. R. *Electrochemical Methods. Fundamentals and Applications*; Wiley: New York, 1980; Chapter 6.

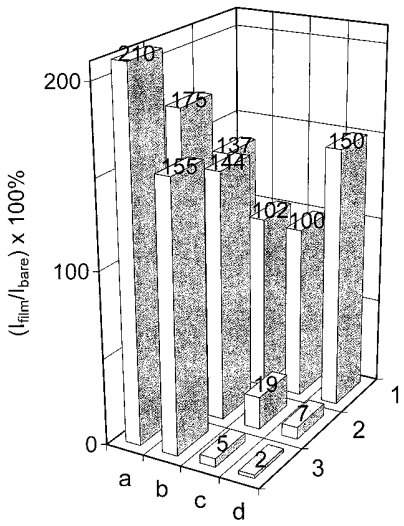

Figure 5. Film permeabilities $P = (I_{film}/I_{bare}) \times 100\%$ (see text). Films: CHIT (1), CHIT-LYVS (2), CHIT-LYVS-GDI (3). Probes: Ru$(NH_3)_6^{3+}$ (a), dopamine (b), ascorbate (c), and Fe$(CN)_6^{4-}$ ions (d).

The increase in α values for the chemically modified chitosan films (Table 1) can be rationalized by the ion-exchange theory.[29] The competition between the Na^+ ions of the background electrolyte and the cationic probe for incorporation into the CHIT-LYVS or CHIT-LYVS-GDI films is decided by the local relaxation free energy of transfer. The free energy of probe transfer between the solution and the film is the result of the stronger interactions (e.g., electrostatic, hydrophobic, etc.) in the solution or the film. The increased preconcentration of Ru$(NH_3)_6^{3+}$ ions into the CHIT-LYVS film can be ascribed to the electrostatic preference of the film for these more highly charged ions. A further increase in α upon the cross-linking of the film with GDI is driven probably by the relaxation of the cross-linked CHIT-LYVS-GDI matrix when three Na^+ ions are exchanged by one Ru$(NH_3)_6^{3+}$ ion. On the other hand, the preconcentration of relatively hydrophobic dopamine $(OH)_2C_6H_3CH_2CH_2NH_3^+$ into CHIT-LYVS film could result from both the electrostatic and hydrophobic interactions of the probe with the anionic LYVS dye. The presence of the hydrophobic GDI cross-links in the CHIT-LYVS-GDI film favors additional hydrophobic interactions with dopamine leading to the increase in α.

The chemically modified chitosan films reject anionic redox probes as illustrated by the decreasing permeabilities shown in Figure 5 (bars 2c,d and 3c,d). Apparently, the presence of the anionic LYVS dye in the CHIT-LYVS film triggers the condition known as Donnan exclusion of co-ions. The electrostatic nature of the exclusion process is supported by the observation that the CHIT-LYVS film rejects more efficiently the higher charged Fe$(CN)_6^{4-}$ ions (bar 2d) than the ascorbate $C_6H_7O_6^-$ ions (bar 2c). A cross-linking of chitosan matrix with hydrophobic GDI molecules further decreases the permeability of the CHIT-LYVS-GDI film to hydrophilic ascorbate (bar 3c) and Fe$(CN)_6^{4-}$ ions (bar 3d).

Permselectivity of Chitosan Films. The permselectivity PE of a film to a cationic analyte over an anionic interference can be expressed as a ratio of permeabilities

$$\mathrm{PE} = P_{\mathrm{cation}}/P_{\mathrm{anion}} \qquad (4)$$

where P_{cation} is the permeability of the Ru$(NH_3)_6^{3+}$ or dopamine $(OH)_2C_6H_3CH_2CH_2NH_3^+$ ions and P_{anion} is the permeability of the Fe$(CN)_6^{4-}$ or ascorbate $C_6H_7O_6^-$ ions. A combination of the two cationic and two anionic probes yields four independent ratios for PE. They can be written as PE(3+/4−), PE(3+/−), PE(+/4−) and PE(+/−) using the probes' charges to shorten the notation. The PE values for the three chitosan films are given in Table 2 , which shows that the film permselectivity increases with the extent of chemical modification of chitosan matrix, i.e., in the order CHIT < CHIT-LYVS < CHIT-LYVS-GDI. This correlates with increasingly slower ionic transport in the film as represented by the decreasing values of D_f (Table 1). Such a correlation is an example of a typical membrane behavior; i.e., the more extensive interactions between the probe and the membrane lead to better chemical recognition of the probe but they slow the probe's transport in the membranes. An attractive feature of the CHIT-LYVS-GDI film as the electrode coating is that it displays a charge-based selectivity in conjunction with a relatively high ion transport. Thus, the chemically modified chitosan is a promising new coating for the development of selective and fast sensors.

Table 2. Permselectivity PE = $P_{\mathrm{cation}}/P_{\mathrm{anion}}$ of Chitosan Films to Cationic Probes Ru$(NH_3)_6^{3+}$ (3+) and Dopamine (+), over Anionic Probes Fe$(CN)_6^{4-}$ (4−) and Ascorbate (−)

film/PE	PE(3+/4−)	PE(3+/−)	PE(+/4−)	PE(+/−)
CHIT	0.9 ± 0.1	1.4 ± 0.2	0.7 ± 0.1	1.0 ± 0.1
CHIT-LYVS	25 ± 4	9.2 ± 1.3	21 ± 3	7.6 ± 1.1
CHIT-LYVS-GDI	105 ± 15	42 ± 6	78 ± 11	31 ± 4

Analytical Performance of Chitosan Electrodes. Flow injection analysis was used to study the analytical performance of electrodes coated with chitosan films. For example, using the amperometric detection at the CHIT-LYVS-GDI electrode (E = 0.60 V), a linear least-squares calibration curve for dopamine over the range 0.010−5.0 mM (6 points) had a slope 17.8 ± 0.6 μA mM^{-1} and a correlation coefficient of 0.996. The detection limit for dopamine was 1 μM using the criterion of a concentration that yielded a signal of 3 times peak-to-peak noise. The response time, defined as time to 90% of the full signal, was 1.8 ± 0.1 s. For comparison, the response time of the bare electrode in our FIA system was 1.4 ± 0.1 s. The latter is considered the maximum response time, because of band broadening in the flow system and filtering of the current data. The CHIT-LYVS-GDI film on the electrode surface was stable during a two-week period of intensive use in the flow system as well as in rotating-disk experiments. After that time, the film was intentionally removed from the electrode surface.

CONCLUSIONS

Chitosan, an amino polysaccharide, is a convenient structural material for the development of functional coatings for electrochemical sensors. Electrode-supported chitosan films display excellent adhesion properties and high mechanical strength and

(29) Fietelson, J. In *Ion Exchange*; Marinsky, J. A., Ed.; Marcel Dekker: New York, 1969; Vol. 2. Ch.4.

stability. An attractive feature of chitosan films is that their molecular design and, thus, physical and chemical properties (e.g., hydrophobicity−hydrophilicity balance) can be custom modified by bonding selected molecules to the amino or hydroxyl groups of the chitosan backbone using simple chemistry. We have built a charge-based chemical recognition into the electrode-supported chitosan films by grafting the anionic Lucifer Yellow VS dye onto the chitosan chains and cross-linking them with glutaric dialdehyde. In addition to good permselectivity against anions, such electrode coatings display a relatively fast ion transport. Consequently, they can be used to design selective and fast-responding electrochemical detectors. In principle, by modifying the chitosan matrix with both selectivity-inducing molecules and redox-active centers, selective and electrocatalytic layers for sensor applications can be envisioned. We are currently investigating chitosan as a biocompatible scaffolding for designing of electrochemical biosensors.

ACKNOWLEDGMENT

This work was supported by the Faculty Research Awards Program at UTSA (W.G.), the Welch Summer Scholarship (J.C.), and the ONR Scholars Program (M.K.). The assistance of Angelica Guerrero in the exploratory part of this study is also gratefully acknowledged.

Received for review August 20, 1999. Accepted December 9, 1999.

AC990954B